

Supporting information

Cation-dependent structural phase transition and dielectric response in a family of cyano-bridged perovskite-like coordination polymers

Wei-Jian Xu, Shao-Li Chen, Zhi-Tao Hu, Rui-Biao Lin, Yu-Jun Su, Wei-Xiong Zhang and Xiao-Ming Chen

†MOE Key Laboratory of Bioinorganic and Synthetic Chemistry, School of Chemistry and Chemical Engineering, Sun Yat-Sen University, Guangzhou 510275, China

■ A brief introduction of MDSC

For a MDSC measurement, the resultant heat flow between the sample and reference is described by a general equation: $dQ/dt = C_p b + f(T, t)$. where dQ/dt is the resultant heat flow, C_p is the capacity of the sample, b is the rate of temperature change (dT/dt), and $f(T,t)$ is the heat flow from kinetic processes. All of these signals are calculated from three measured signals: time, modulated temperature, and modulated heat flow. The total heat flow is calculated from the average of the modulated heat flow; the reversing heat flow ($C_p b$) is then calculated by multiplication of C_p with the negative heating rate b ; the non-reversing heat flow ($f(T, t)$) is the arithmetic difference between the total heat flow and the reversing heat flow.

Table S1. Summary of crystal data and structural refinements for compounds **1–4** at different temperatures.

Compound	1	2	3	4				
Formula	[CH ₃ NH ₃] ₂ [KFe(CN) ₆]	[(CH ₃) ₂ NH ₂] ₂ [KFe(CN) ₆]	[(CH ₃) ₃ NH] ₂ [KFe(CN) ₆]	[(CH ₃) ₄ N] ₂ [KFe(CN) ₆]				
T (K)	193(2)	443(2)	165(2)	298(2)	113(2)	350(2)	298(2)	373(2)
Crystal system	monoclinic	Cubic	Tetragonal	Tetragonal	monoclinic	Cubic	Tetragonal	Cubic
Space group	<i>C</i> 2/c	<i>F</i> m-3 <i>m</i>	<i>P</i> 4/mnc	<i>P</i> 4/mnc	<i>C</i> 2/c	<i>F</i> m-3 <i>m</i>	<i>I</i> 4/ <i>m</i>	<i>F</i> m-3 <i>m</i>
<i>a</i> /Å	13.702(3)	11.4771(2)	8.2769(4)	8.3102(1)	15.3805(3)	12.104(2)	8.843(2)	12.451(2)
<i>b</i> /Å	7.9005(2)	11.4771(2)	8.2769(4)	8.3102(1)	8.4336(1)	12.104(2)	8.843(2)	12.451(2)
<i>c</i> /Å	13.703(3)	11.4771(2)	11.6742(8)	11.684(3)	13.8970(2)	12.104(2)	12.150(4)	12.451(2)
β°	108.642(6)	90	90	90	107.583(3)	90	90	90
<i>V</i> /Å ³	1405.5(6)	1511.8(3)	799.77(9)	806.9(3)	1718.4(4)	1773.2(5)	950.1(4)	1930.1(6)
<i>Z</i>	4	4	2	2	4	4	2	4
<i>D</i> _c /g cm ⁻³	1.490	1.385	1.425	1.413	1.435	1.391	1.396	1.374
reflns coll.	7552	3325	4156	5089	13728	4120	4816	3714
unique reflns	1602	121	419	498	1970	136	566	147
<i>R</i> _{int}	0.0280	0.0584	0.0395	0.0268	0.0223	0.0310	0.0292	0.0301
<i>R</i> ₁ [<i>I</i> > 2σ(<i>I</i>)]	0.0322	0.0618	0.0678	0.0314	0.0247	0.0369	0.0328	0.0239
<i>wR</i> ₂ [<i>I</i> > 2σ(<i>I</i>)]	0.0754	0.1863	0.1761	0.0853	0.0578	0.0977	0.0875	0.0673
<i>R</i> ₁ (all data)	0.0330	0.0618	0.0700	0.0359	0.0250	0.0370	0.0334	0.0250
<i>wR</i> ₂ (all data)	0.0766	0.1863	0.1776	0.0891	0.0580	0.0978	0.0881	0.0675
GOF	1.097	1.196	1.067	1.064	1.030	1.182	1.138	1.072

^a*R*₁ = $\sum \|F_o\| - |F_c\| / \sum |F_o|$, *wR*₂ = { $\sum w[(F_o)^2 - (F_c)^2]^2 / \sum w[(F_o)^2]^2$ }^{1/2}

Table S2. Selected bond lengths and Fe \cdots K distances (\AA) for **1–4** at α and β phases.

Phase	Fe-C	K-N	C-N	Fe \cdots K
1α	1.938(2)	2.823(2)	1.147(2)	5.4144(8)
	1.937(2)	2.854(2)	1.151(2)	5.5732(9)
	1.948(2)	2.889(2)	1.151(2)	5.8312(9)
1β	1.930(2)	2.832(2)	1.083(2)	5.7385(8)
2α	1.971(7)	2.942(7)	1.126(1)	5.8527(2)
	1.937(10)	2.759(10)	1.141(14)	5.8371(4)
2β	1.944(3)	2.934(2)	1.140(3)	5.8761(7)
	1.932(4)	2.773(4)	1.137(5)	5.842(2)
3α	1.960(5)	3.174 (5)	1.153(7)	5.8730(4)
	1.946(1)	2.874(1)	1.152(7)	5.9153(5)
	1.948(1)	2.835(1)	1.149 (8)	6.2263(5)
3β	1.933(5)	3.000(7)	1.184(1)	6.052(1)
4α	1.955(4)	3.190(2)	1.150(4)	6.253(1)
	1.959(3)	2.971(2)	1.150(3)	6.075(2)

Table S3 The dipole moment of cations guest and each cage in **1–4**.

compound	$\mu_{\text{cations}} / \text{Debye}$	$\mu_{\text{cage}} / \text{Debye}$	$\mu_{\text{total}} / \text{Debye}$
1	2.2	5.7	7.9
2	1.5	4.1	5.6
3	0.8	2.3	3.1
4	0	0	0

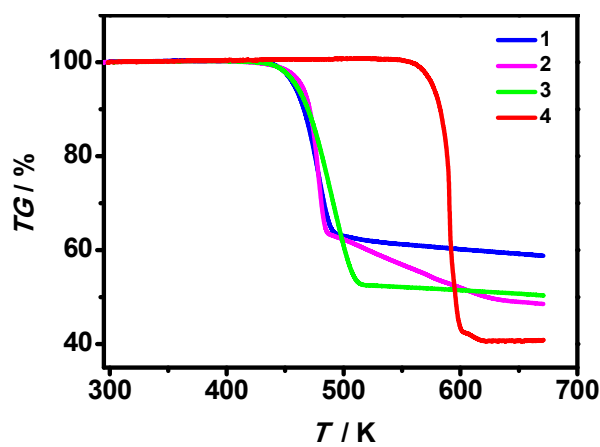


Fig. S1. TG profiles of **1–4**.

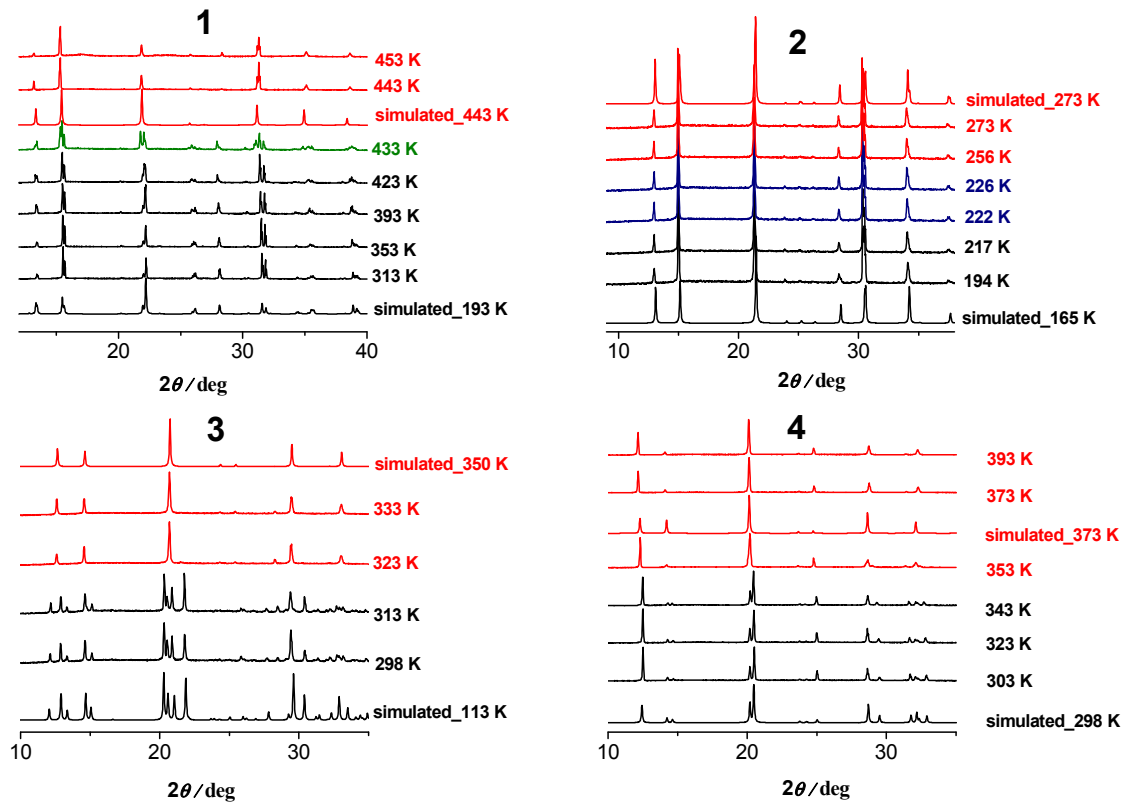


Fig. S2. The variable-temperature powder X-ray diffraction patterns of **1–4**.

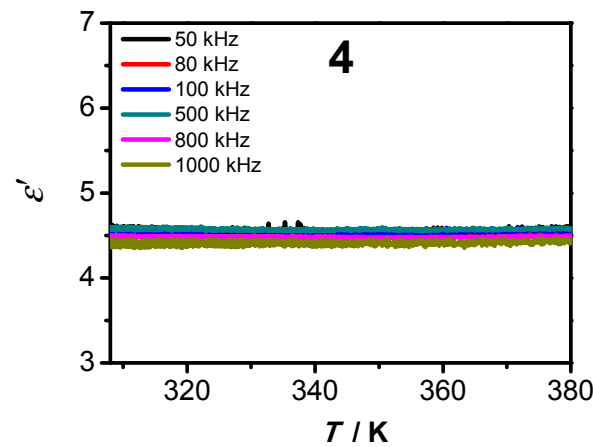


Fig. S3. Temperature-dependent dielectric constant of **4**.

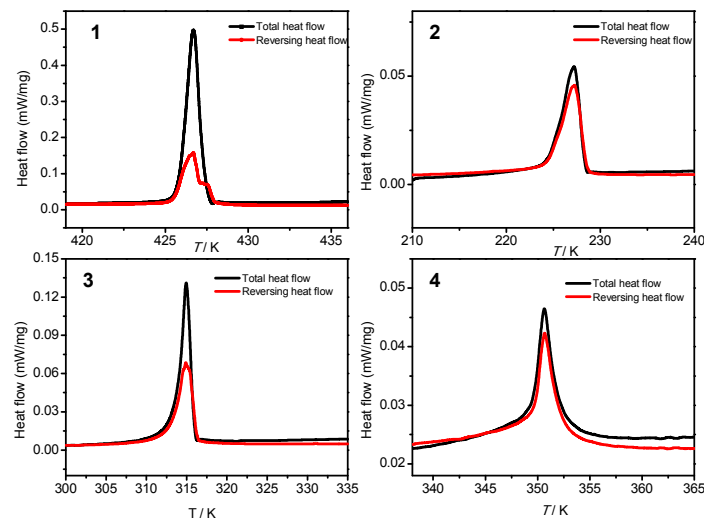


Fig S4. Reversing heat flow and total heat flow for **1–4**.

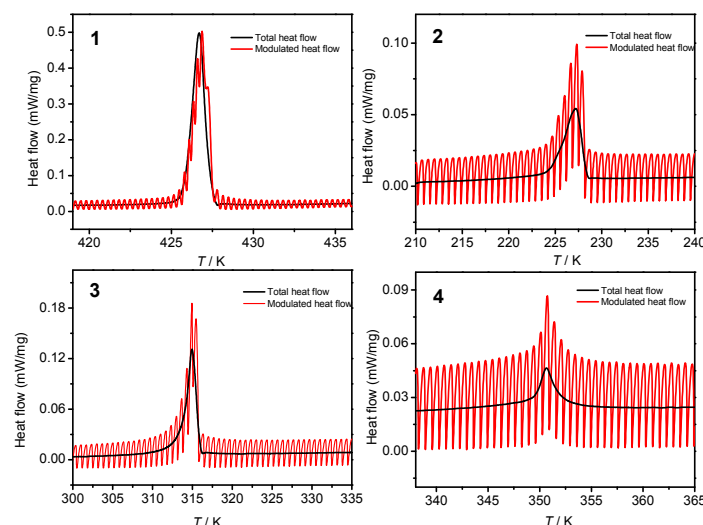


Fig. S5. Modulated heat flow and total heat flow for **1–4**.

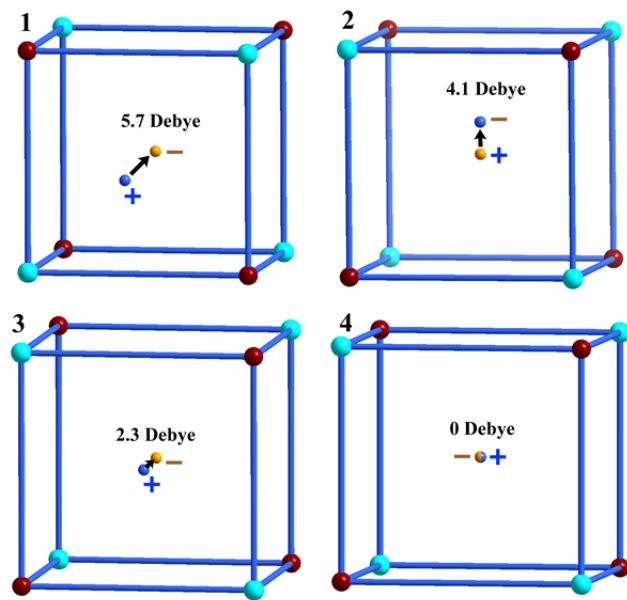


Fig. S6. The dipole moment produced by the separate positive-negative point charge of each cage in 1–4.